ON THE SPATIAL AND TEMPORAL VARIATION OF GLM FLASH DETECTION AND HOW TO MANAGE IT

POSTER 692

Kenneth L. Cummins[1]
University of Arizona, Tucson, AZ 85721

1. INTRODUCTION

Data from the Geostationary Lightning mapper (GLM) on the GOES-16 satellite have been employed extensively in both research and operations since the instrument's certification in November 2018. Efforts continue to better understand and describe the performance of GLM for both the GOES-East and GOES-West locations, with the objective of assuring informed use of these important datasets.

The fraction of flashes reported by GLM on GOES East has been shown in earlier studies to be much lower in northwest CONUS than in the southeast. Comparisons of GLM detection in the GOES-East location with three independent datasets was carried out by Blakeslee et al. (2020) and is shown in Fig. 1. The work presented here demonstrates that this behavior is part of a broader dependence of detection on GLM pixel thresholds that increase steadily from the center to the edges of the field-of-view (FOV), modulated by local day:night differences in threshold, which is a known design constraint. This relationship allows us to predict GLM performance at any location in the FOV, with the potential to provide real-time information about GLM performance to help in the assessment of specific storms using tracking of GLM pixel thresholds. It also provides a quantitative means to optimize a "merged" GLM dataset where GOES-East and West coverage overlap.

In this work, detection is evaluated using the Kennedy Space Center and Colorado Lightning Mapping Arrays (KSCLMA and COLMA, respectively). The inputs for model estimates of performance are derived from long-term observations by the Lightning Imaging Sensors (LIS) on the TRMM satellite and on the International Space Station (ISS).

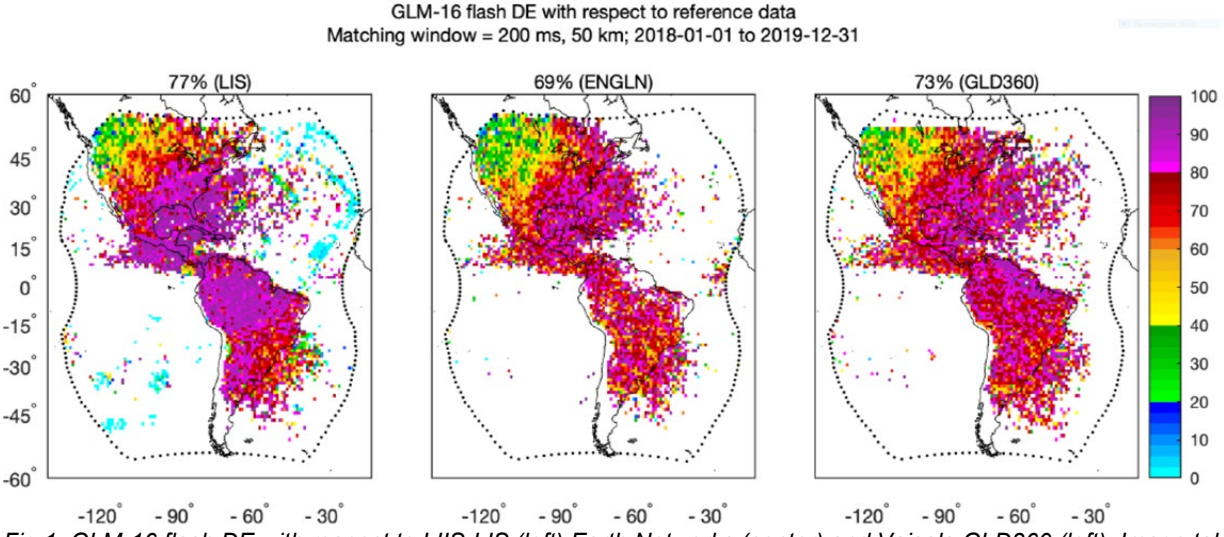

Fig.1. GLM-16 flash DE with respect to LIIS-LIS (left) Earth Networks (center) and Vaisala GLD360 (left). Image taken from Blakeslee et al. (2020)

[1] *Corresponding Author Address:* Kenneth L. Cummins, University of Arizona, Dept. of Hydrology & Atmospheric Sciences, Tucson, AZ 85721; e-mail: kcummins@arizona.edu

2. DATASETS

2.1 Geostationary Lightning Mappers (GLM)

GLMs are on both GOES-16 (GOES-East, centered at 75 W) and GOES-17 (GOES-West, centered at 137 W) satellites with a latitude coverage of ± 54º (Rudlosky et al., 2019). GLMs are designed to measure radiation signals at 777.4 nm (with a 1 nm bandwidth) from transient lightning discharges and strokes in intra-cloud (IC) and cloud-to-ground (CG) flashes. The sensor has a wide FOV with a 1372×1300 pixel Charge Coupled Device (CCD) array at the focal plane (Goodman et al., 2013). The array has larger pixels in the center and smaller pixels near the edges in order to create a near-uniform spatial resolution (~8 km) in the central 2/3 of the FOV, doubling in area near the useful edge of the FOV. Several recent publications describe GLM products and performance characteristics (Bateman & Mach, 2020; Blakeslee et al., 2020; Mach, 2020; Murphy & Said, 2020; Rutledge et al., 2020; Thomas et al, 2019; Zhang & Cummins, 2020).

2.2 Lightning Imaging Sensor (LIS)

Two different LIS instruments were used in this study. Lightning information from 2012 and 2013 was obtained by LIS onboard the low Earth orbital Tropical Rainfall Measuring Mission (TRMM) satellite, which orbited at 35º inclination. LIS made approximate 90 second observations for any single location on Earth during an overpass. Similar to GLM, LIS is also an optical sensor, but with 128 × 128 pixels in the array and the pixel size of LIS is about 4 km near the center of the array, roughly doubling near the edges of the array. LIS also has the same main three levels of products as GLM (event, group, and flash). A recent detailed assessment of TRMM LIS and its products is provided by Zhang et al. (2019) and the references therein. After 17 years on orbit, TRMM-LIS ended its service in 2015. This led to placement of a second LIS instrument on the ISS to provide simultaneous comparisons between LIS and GLM (Blakeslee et al., 2020). ISS-LIS provides lightning observations between +/- 55º latitudes with similar spatial resolute as TRMM-LIS. This study employs ISS-LIS data from 2018 and 2019. The LIS datasets are well-matched sources to help understand the nature of cloud-top optical sources from lightning and their regional differences.

2.3 Lightning Mapping Array (LMA)

The LMAs at KSC and in Colorado locate the impulsive very high frequent (VHF) breakdown processes (sources) produced during a lightning flash by measuring the time of arrival of the electromagnetic radiation signals using 5 or more stations (Thomas et al., 2004). LMA's ability for mapping the fine structure of lightning with high accuracy has led it become the "ground-truth" dataset in this study. For this work, the LMA's were assumed to report and accurately characterize the spatial and temporal extent of all flashes. This may not be the case for KSC, since the KSCLMA only had eight operational sensors during much of the study period. Analyses of several LMA systems by Chmielewski and Bruning (2016) indicates that it is fair to assume that at least 95% of all flashes within 100 km of the center of a properly maintained LMA system will be reported. The use of LMA to determine flash characteristics and assess GLM detection is described in detail in Zhang and Cummins (2020). Representative findings at KSC illustrating DE as a function of LMA-derived flash parameters are shown in Fig.2.

3. MODELING AND RESULTS

3.1 GLM Detection Efficiency Modeling

The modeling approach used in this work follows the conceptual framework described in Boccippio et al. (2002). Assessment of lightning detection by GLM is conceptually very simple. If the accumulated optical energy over the ~2 ms "frame time" incident on a GLM pixel exceeds that pixel's energy acceptance threshold, then the event is detected. Much goes into getting enough light onto a tiny pixel 22,000+ miles above the earth and holding the imager still enough to register and geolocate this energy. Also, there are numerous factors that influence the amount of light at cloud-top produced by current in a lightning channel, compared to the sunlight reflected upward by the same cloud and/or the inherent noise in the instrument. However, this work only deals with characterizing the conditions under which the lightning-related optical energy at a GLM pixel is above its acceptance threshold.

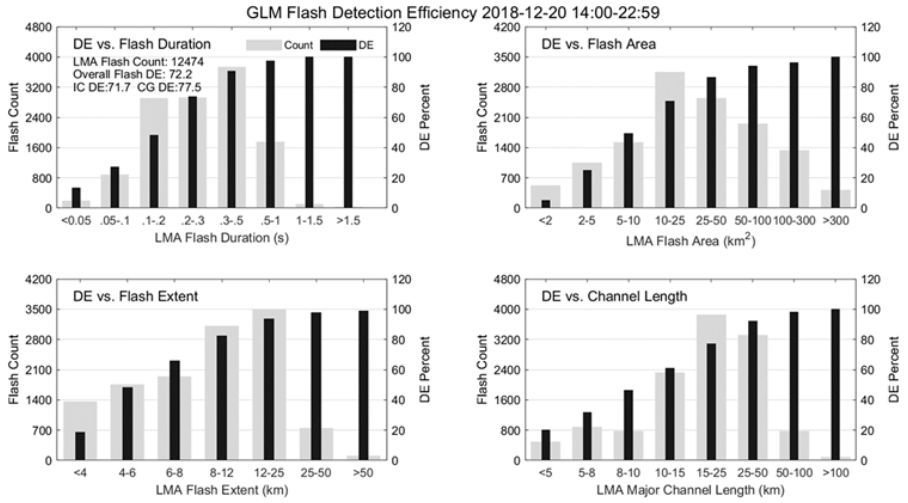

Fig 2. GLM Detection Efficiency (DE) as a function of various LMA flash parameters for eight hours of storms near KSC on December 20, 2018. Note that DE varied between 10 and 100% as a function of flash size (area, duration, and channel length). See Zhang and Cummins (2020) for further details.

It should be noted that this work, unlike the detailed analysis carried out by Boccippio et al. (2002), employs detection threshold in terms or energy rather than spatial energy density. Energy is the parameter that determines the signal amplitude that is compared to a physical instrument threshold. When evaluating a single instrument or comparing instruments with similar designs and pixel sizes, it is not unreasonable to interchangeably employ energy or spatial energy density, since they are related by a nearly constant area. However, here the LIS instruments are used to establish optical source characteristics for GLM with a nominal factor-of-2 difference in pixel dimension (factor-of-four in area). By using energy and by directly addressing source- and pixel-size issues, a more-direct and precise analysis can be carried out. An additional motivation to use energy is that GLM threshold is directly provided in terms of incident energy.

The following sections describe the spatial and temporal behavior of GLM instrument thresholds, and the cloud-top optical energy as seen by satellites. Detection modeling based on these observations is then compared to assessments using LMA systems in Florida and Colorado. The model is then used to estimate flash DE from GOES-East and GOES-West locations, with a closer look at their overlapping areas in North America. Lastly, the ability to measure and track GLM threshold using the operational “L2” GLM dataset is demonstrated in Colorado, with the thought that this demonstration might lead to threshold tracking in real-time to support operational interpretation and research applications of GLM data.

3.1.1 GLM Threshold

At any instant in time, every pixel in a GLM instrument is assigned a detection acceptance threshold (in units of fJ) that is determined by its viewing geometry and by the background “noise” level just prior to that time. As currently configured, the minimum threshold occurs at the nadir viewing angle, and is about 1 fJ measured at the image plane within the instrument. This nominal threshold increases to more than 20 fJ at operationally relevant locations near the edge of the FOV. Each pixel has several possible threshold values, where the range between the minimum and maximum threshold is typically about a factor-of-two. The specific threshold for any given GLM pixel is determined by the recent background illumination level which is influenced by the solar reflection from earth/ocean/cloud volumes, and potentially by lightning-related illumination during high flash-rate storms.

The set of possible threshold values for each pixel can be derived directly from the GLM L2 event data. For convenience, Lockheed Martin has provided this information on a restricted (but not confidential) basis, and these data were used in the analyses provided in this paper. Illustrative threshold values are shown in Fig. 3.

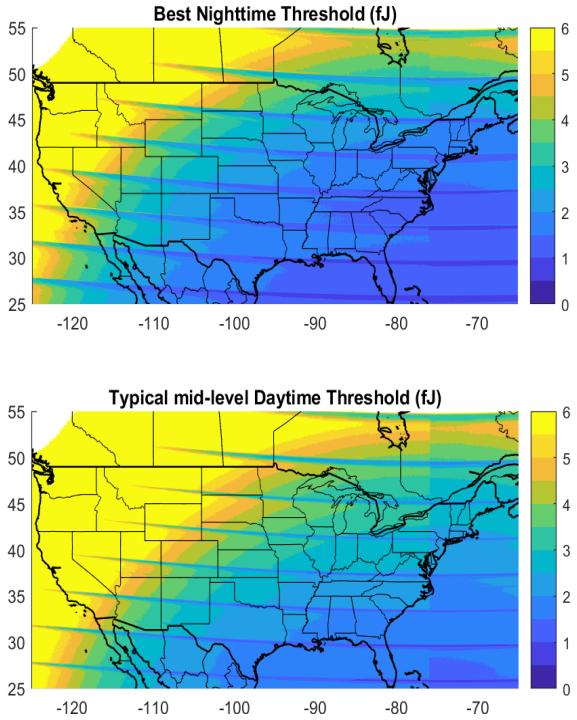

Fig. 3. Representative GLM threshold values for the CONUS domain of GOES-East.

The "Best Nighttime" values reflects the minimum threshold condition for each GLM pixel. The "Typical mid-level" values are a mid-level threshold that should reflect typical daytime values. The horizontal bands of locally-low threshold values are found near the boundaries between GLM image processing units, are the result of a signal processing limitation in the first two GLM sensors on GOES-16 and -17. This issue has been addressed in the other two GLM sensors to be deployed at later dates (Kpulun et al., this conference).

3.1.2 Cloud-top Optical Energy Distributions

The influence of GLM detection threshold on detection efficiency is determined by the "brightness" of lightning-produced cloud-top optical sources, expressed here as the satellite-measured optical energy seen by a GLM pixel. Recent work by Zhang and Cummins (2020) and Quick et al. (2020) has shown that most of these sources are smaller than a GLM pixel (~64 km^2), with many of them exhibiting GLM-equivalent energy values below at or below 1 fJ. The expected optical pulse energy and "size" also varies with time-in-flash, and therefore with flash durations and flash size (Zhang and Cummins, 2020).

In this work, we explore GLM-equivalent cloud-top optical energy by region using the two LIS instruments. These instruments provide the only known long-term datasets to obtain consistent regional estimates of cloud-top energy that can be directly related to GLM detection. More-specifically, LIS group radiance, area, and event count are used to produce GLM-equivalent optical energy estimates using the technique described by Zhang and Cummins (2020). The subset of the highest-energy reports in each LIS flash are used to directly estimate the fraction of LIS flashes that would be reported by GLM.

Fig. 4a shows the energy distribution for the highest-energy TRMM-LIS groups for each flash within the LIS view of CONUS (below 38° N latitude) in 2013. The data are aggregated as a function of the number of LIS events in eaxh group. Cumulative distributions are shown for the sub-populations of group sizes. The sub-group for up to four events (cum14) is a crude approximation to the size of a GLM pixel, assuming that a GLM pixel (~8x8 km) is about 4x larger than the typical LIS pixel (4-5 km on a side). The estimates of GLM DE presented in the poster associated with this extended abstract employed this "optical source distribution." This distribution was shown to underestimate DE at higher thresholds. It also under-represented the fraction of GLM "flash-max" events (maximum energy event in flash) for the KSC study, shown in Fig 4b, which indicate that 10 percent of the flash-max events had energy values above 20 fJ.

Further work to address these shortcomings has resulted in the "GLM-like" cumulative distribution (red curve) shown in Fig. 4a, which is constructed as follows. Three max-energy values were computed for each flash: (1) total group energy; (2) highest energy LIS pixel; and (3) the total group energy divided by the group area (fJ/m^2) multiplied by the nominal area of a GLM pixel (64 km^2). One of these energy values was selected to represent the flash's brightest "GLM-equivalent" optical source (event), selected as follows. For LIS groups with fewer than three events, the total group energy was selected, assuming that the true optical source was smaller than a GLM pixel. For LIS groups with 3 or more events, the larger of the other two max-energy values was selected, accommodating the possibility of either a

small-but-bright source or a large-but-uniform source. It is not difficult to find conceptual limitations with this approach, but the "fit" with the observed GLM max-event distribution shown in Fig. 4b is compelling.

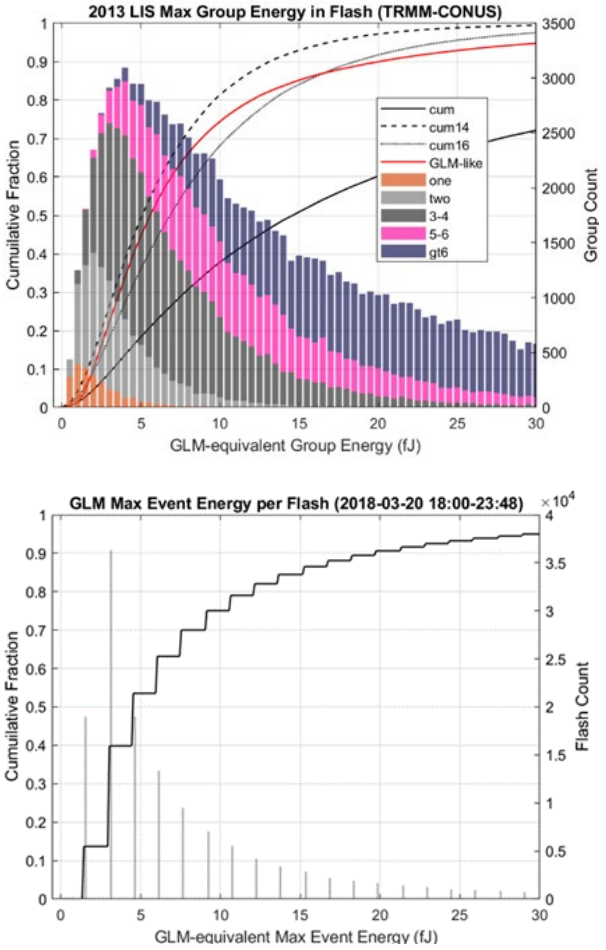

Fig. 4. (a) Group Energy distributions for "highest energy group in each flash." With the TRMM domain for CONUS. The distribution is subdivided by the number of events in these groups for groups containing one, two, 3-4, 4-6, and gather than 6 events (gt6). Cumulative distributions of energy for 1-4, 1-6, and all groups are shown as black curves. The "GLM Estimate" cumulative curve is shown in red and is described in the text. (b) Histogram and cumulative distribution for the highest energy event in all flashes reported by GLM during the 2018-19 study period at KSC. The 1.5 fJ "quantization" of energy is due to the energy resolution for that GLM dataset.

An additional complication is regional and inter-annual differences in the long-term optical source distributions. This was explored in a two-step process. First, the interannual variability of source distributions was compared for two TRMM-LIS years (2012 and 2013) and two ISS-LIS years (2018 and 2019) for a region covered by both instruments. Next, regional differences were evaluated. Regional differences are expected, based in land:ocean and regional differences noted by Chronis and Koshak (2017) and Beirle et al. (2014). Fig. 5 shows the GLM-equivalent event energy distributions for the TRMM-LIS CONUS domain for TRMM-LIS in 2012 and 2013, and for ISS-LIS in 2018 and 2019. This domain is the region bounded by latitudes between 25 and 38° N and by longitudes between 65 and 125° W, so the oceanic region includes the Atlantic gulf stream, much of the Gulf of Mexico, and a small portion of the western pacific coastal waters. These distributions do not differ by more than 2% over the range of 0-30 fJ and are within 1% of each other above 30 fJ. Therefore single-year distributions can be employed, and data from TRMM and ISS instruments can be viewed as equivalent.

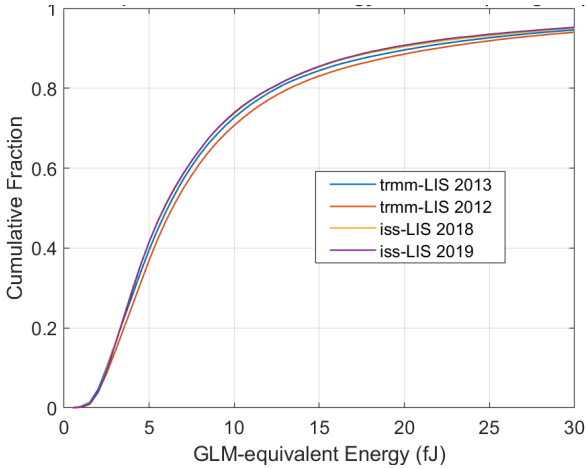

Fig. 5. GLM-equivalent event energy for the TRMM-LIS CONUS domain for four years. TRMM-LIS was used in 2012-2113, and ISS-LIS was used in 2018-2019.

Fig. 6 shows the GLM-equivalent event energy distributions for three regions for ISS-LIS in 2018 and 2019. ISS-LIS was used because of its coverage above 38° North. The pairs of within-region distributions differ by less than 2%, with the largest difference being in Colorado for the coverage-region for COLMA. This variability is likely due to the modest annual number of flashes in this region, leading to some inter-annual variability. There is considerable variation between regions, with the lowest median value in Colorado (~5 fJ) and a 60% higher median value in the southeastern U.S. (~8 fJ).

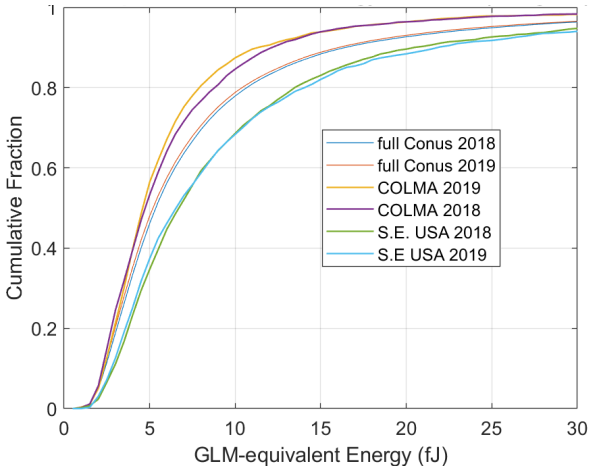

Fig. 6. GLM-equivalent event energy for ISS-LIS in three different regions.

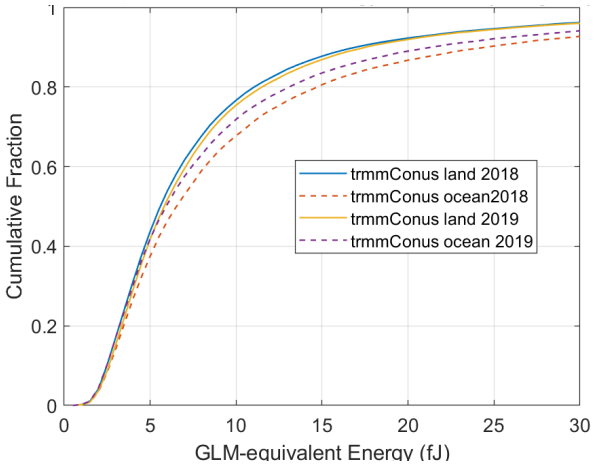

Fig. 7. GLM-equivalent event energy for ISS-LIS over CONUS land and over nearby oceanic areas.

The "full Conus" curves match quite well with the estimated "GLM Pulse Detection Efficiency" curve derived using observations obtained by the Fly's Eye GLM Simulator during GOES-R validation (Quick et al., 2020; see their Fig. 10).

The COLMA region curves likely reflect the impact of two behaviors of thunderstorms east of the front range in Colorado. Anomalously electrified storms are common in this region, and these storms exhibit high lightning flash rates and low flash heights relative to cloud depth (Rutledge et al., 2020). Additionally, high flash rates are typically associated with small flash sizes and durations (Bruning and MacGorman, 2013). All of this leads weaker cloud-top optical energy than is found in storm in other regions with more traditional charge structures.

A land:ocean energy comparison over the TRMM-LIS CONUS domain is shown in Fig. 7. The land-only distributions for the two years are nearly identical. There are up to 2% differences between the oceanic regions for these two years, but both curves indicate much higher optical energy over the oceanic regions than over land, consistent with earlier work. These findings suggests that locally derived optical source distributions should be considered when estimating GLM detection over wide geographical areas.

One additional processing step was required to accurately represent the optical source distributions for GLM. To date, GLM does not report a lightning flash unless it has produced at least two optical groups – either as spatially separated optical pulses during the same 2-ms period, or as temporally separated optical pulses (two different 2-ms periods) in close spatial proximity *(personal communication, Doug Mach, 2020*). This condition can be emulated by using the optical source distribution for the second-brightest group in a flash. Fig. 8 shows the GLM-equivalent event energy distributions derived from first- and second-brightest groups in LIS flashes for the full CONUS region employed in Fig. 6. The 2018 and 2019 curves are almost indistinguishable. The GLM-equivalent energy for the brightest group has a median value just above 5 fJ, whereas the 2nd - brightest group median is about 4.5 fJ. The two conditions exhibit the largest difference at threshold (about 1 fJ), indicating that about 8% of the LIS flashes did not have a detectable second group. The curves become indistinguishable above 16 fJ.

3.2 *Model Verification and Testing*

Modeled GLM flash detection was compared to actual performance relative to the Lightning Mapping Array near KSC using more than 20 storm-days during an 11-month period in 2018-19. The optical source distribution used in the model was derived from ISS-LIS in 2018 for the southeastern U.S land mass bounded by latitudes between 25 and 35° N and by longitudes between 77 and 90° W. This larger region was used in order

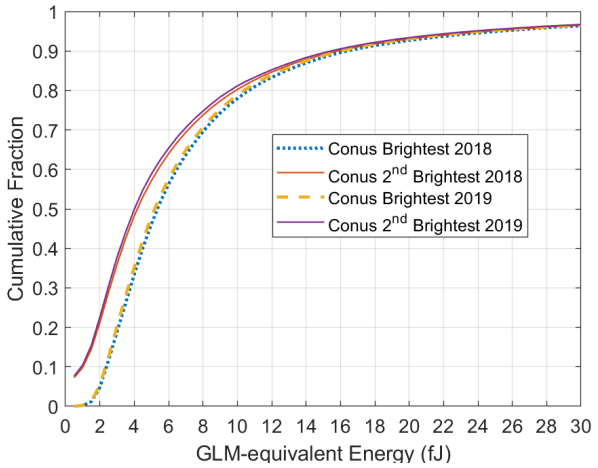

Fig. 8. GLM-equivalent event energy (brightest and 2nd-brightest) for ISS-LIS over the TRMM-CONUS region in both 2018 and 2019.

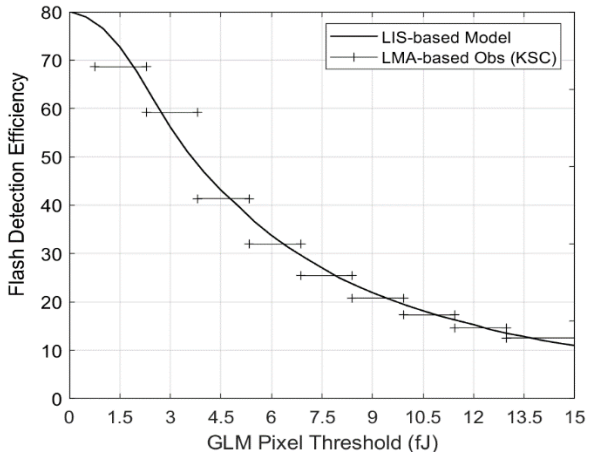

Fig. 9. Modeled and measured GLM flash detection efficiency as a function of GLM detection threshold.

to avoid LIS sampling limitations for small regions. Consistent with the GLM requirement for at least two groups in a flash, the distribution for the 2nd-brighttest source was used.

Verification results are shown in Fig. 9. The LMA-based flash DE for GLM for this dataset was 69%, reflected in the horizontal bar centered on 1.5 fJ, which is the quantization resolution for the GLM energy values during this study period. The decreasing "observed" DE values at higher thresholds were produced by eliminating flashes who's brightest GLM event energy was below the corresponding value. The modeled DE (smooth curve) was scaled to a maximum of 80% to obtain the best visual match. This value is consistent with day/night estimates of 73/94 percent (respectively) by Boccippio et al. (2002). The agreement between the modelled and observed DE is quite good for all threshold values. It is worth noting that DE estimates using optical source distributions for other regions, as well as for this southeastern U.S. region including the nearby ocean area, were all poorer fits to the observed performance near KSC.

3.3 *Threshold-based Model*

Considering the insights derived from the analyses described above, it is possible to produce reasonable estimates of flash DE with quantified uncertainty throughout the fields-of-view for the GLM instruments on GOES-East and -West, as shown in Fig. 10. The assumed conditions are as follows. The threshold information is taken directly from tables provided by Lockheed Martin, using the lowest threshold for each GLM pixel for nighhtime detection and a mid-level threshold for daytime detection. The optical source distribution is for "full Conus 2019", which falls about halfway between the distributions for the southeastern U.S. and the Colorado (COLMA) regions, all shown in Fig. 6. The "2nd Brightest" source distribution was used, to be consistent with the current GLM flash reporting configuration. Finally, the LIS flash detection is assumed to be 80%, consistent with the value found during model verification at KSC (see Fig. 9).

Interpretation of these "nominal" DE maps should be colored by the understanding that the distribution of optical sources varies somewhat by region. The maximum impact of this behavior can be inferred within CONUS from an inspection of Fig. 3 that that depicts regional threshold differences, and Fig. 6 that depicts the most-extreme range of source distributions in the U.S. For example, the daytime threshold in Colorado is 4-5 fJ (Fig. 3). If the 5 fJ "line" is used to explore the likely difference in source distributions between "COLMA" and "Full CONUS" in Fig. 6, the difference is about 10%. Therefore, the actual flash DE in Colorado can be expected to be about 10% lower than the value shown in Fig. 10. Similarly, the daytime threshold in the southeastern U.S. (Florida) is about 1.5 fJ (Fig. 3). The difference in source distributions between "S.E. USA" and "Full CONUS" in Fig. 6 is less than 10%, with the S.E. USA having brighter sources. Therefore, the actual flash DE in Florida can be expected to be no more than 10% higher than the values shown in Fig. 10.

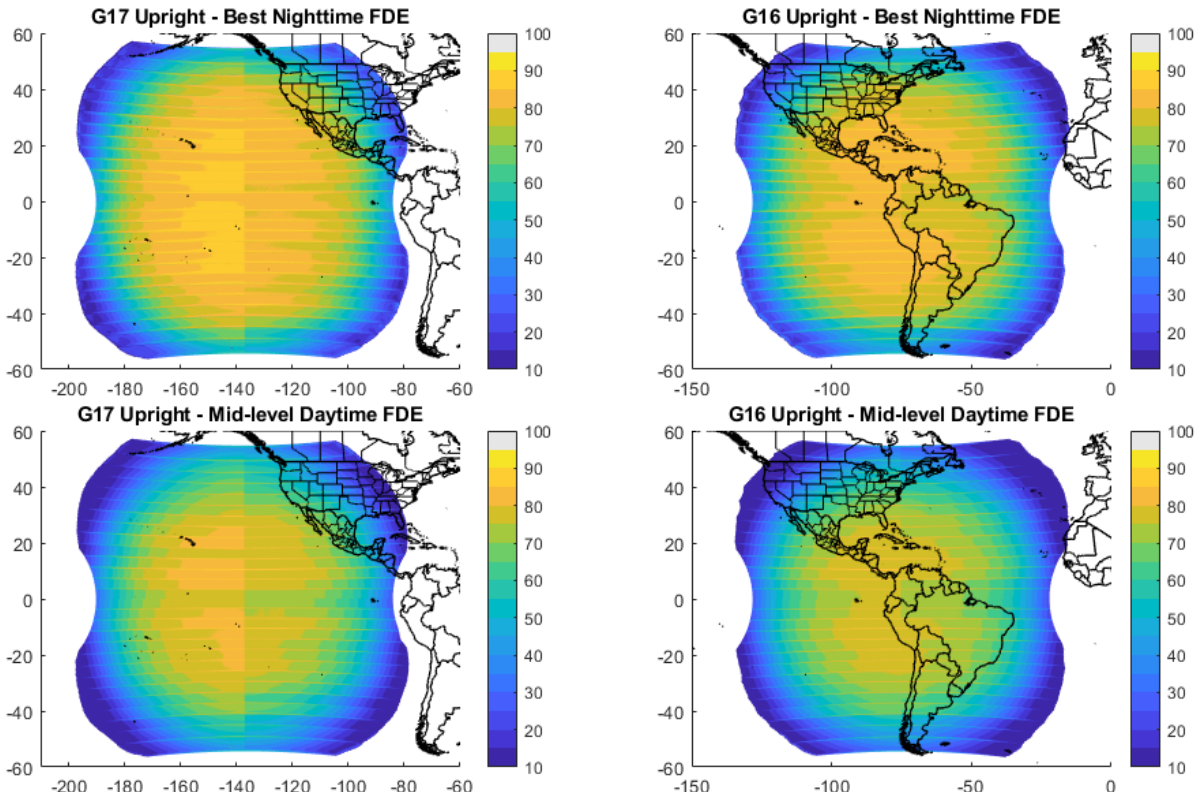

Fig. 10. Estimated GLM flash detection efficiency for GOES-East (G16) and GOES-West (G17) based on known GLM thresholds, full-CONUS distribution of estimated optical source energies, and an assumed ISS-LIS DE of 80% based on model verification at Kennedy Space Center, Florida.

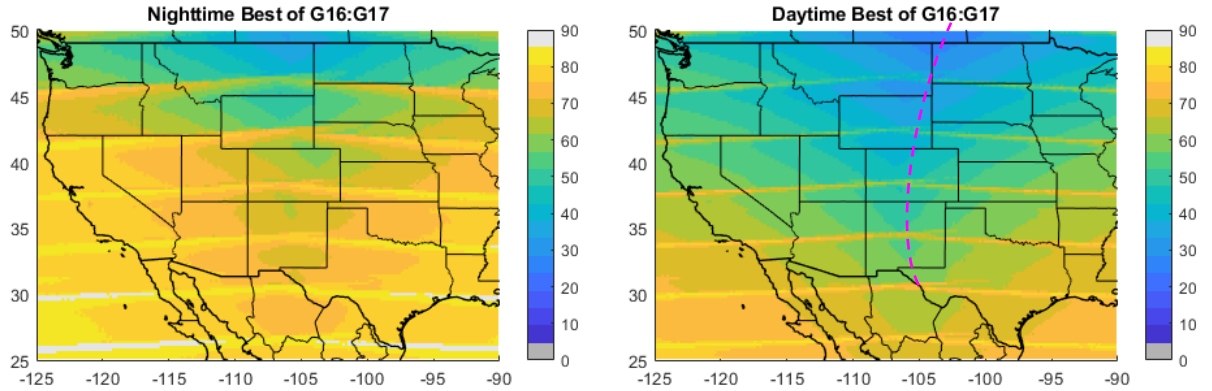

Fig. 11. Daytime and nighttime flash detection efficiency estimates for the western and central U.S. derived from the "best-DE" satellite. The dividing-line between the choice between GLM on GOES-East and -West, based on the modeling presented here, is shown as the magenta dashed line in the right panel.

Future work will focus on using local optical source distributions to produce estimates of flash DE, but the images in Fig. 10 provide very helpful initial information that can be put to use immediately.

3.4 *Best-case Coverage*

One practical question related the use of GLM data is the choice between the GOES-East and -West datasets. Assistance with this choice is provided in Fig. 11, where the best (estimated) DE is shown for the western 2/3 of the U.S. The magenta dashed line in the right panel shows the "dividing line" for best west:east performance. The choice between GLM on GOES-East and -West, based on the modeling presented here, can be a somewhat "lose" because the transition occurs over

a rather large east:west domain. There might be "second order" effects related to pixel threshold that are due to different background scenes viewed from the two satellite locations that is not addressed in this analysis.

It is also important to note that neither satellite provides good coverage during daylight hours in the upper central plains, particularly for much of Montana, North and South Dakota, Wyoming, and northern Colorado.

3.5 *Threshold Tracking*

Given the sensitivity of DE to thresholds above about 2.5 fJ, and the fact that threshold within a region can vary by a factor-of-two due to background illumination, there will be times in the western U.S. when short-term threshold variations can alter DE for an ongoing storm by more than 50%. The best mitigation for this problem will be to reduce the threshold variations, which is likely to be addressed in the next two instruments in the GOES-R series (Kpulun et al., 2021). In the meantime, it will likely be useful to have real-time information about threshold variations for ongoing storms, with some inobtrusive way to report the compromised condition. Toward this end, methods to track local threshold variations using operational GLM data are being explored. An example case-day analysis for storms in Colorado (May 20,2020) is provided below. Fig. 12 shows the domain for this analysis, and the per-pixel GLM (GOES-East) minimum and maximum thresholds throughout the 6-hour evolution and propagation of several multicellular storms. Storm propagation was nominally west-to-east, starting during full daylight and continuing to full darkness. Threshold values were typically 5-7 fJ in the west, due to storms occurring before sunset in that region. Threshold values were typically 2.5-4.5 fJ in the east, where much of the lightning occurred after sunset and into the night. Fig. 13 provides a time series of related parameters for the complete 6-hour period, with statistics accumulated in 2-minute intervals. The per-minute flash rate in the region is represented by the light gray bars. During the 40-minute period prior to the peak rate at 00 UTC, the flash rate steadily increased from less than one per minute to 500 per minute. During this period, the flash DE decreased from about 40% to about 5%, and the median GLM threshold (green line) was greater than 6 fJ. Over the next 3 hours, then median GLM threshold decreased steadily down to about 3 fJ and the flash DE increased steadily back to 40%. Just prior to 03:30 UTC, GLM flash DE exhibited an increasing trend that co-varied with a decrease in the percentage of flashes that were smaller than 10 km^2 (magenta line) as determined by COLMA. These findings demonstrate the strong influence of GLM threshold on flash detection in this region and the ability to track this threshold over time.

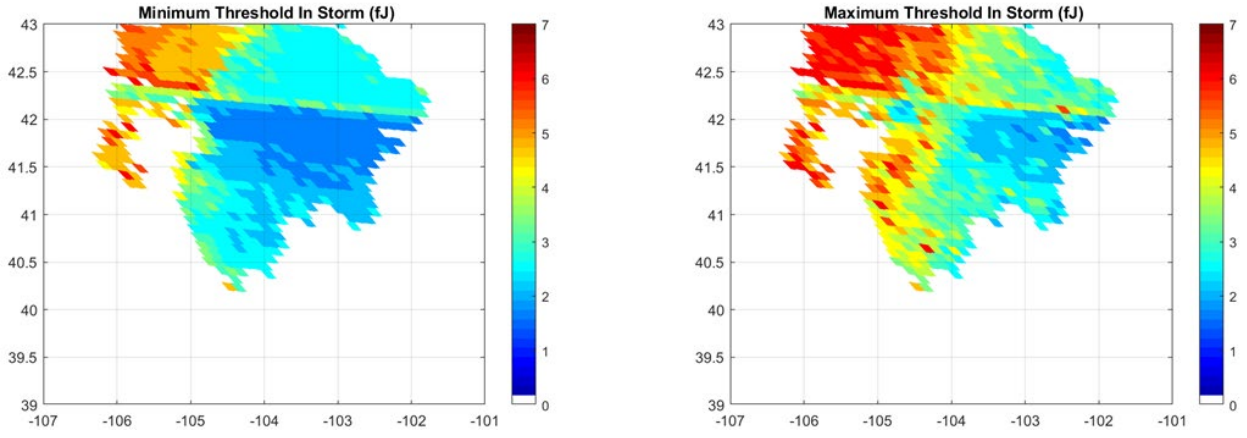

Fig. 12. Minimum and maximum threshold (fJ) through the Colorado storm case on May 20,2020.

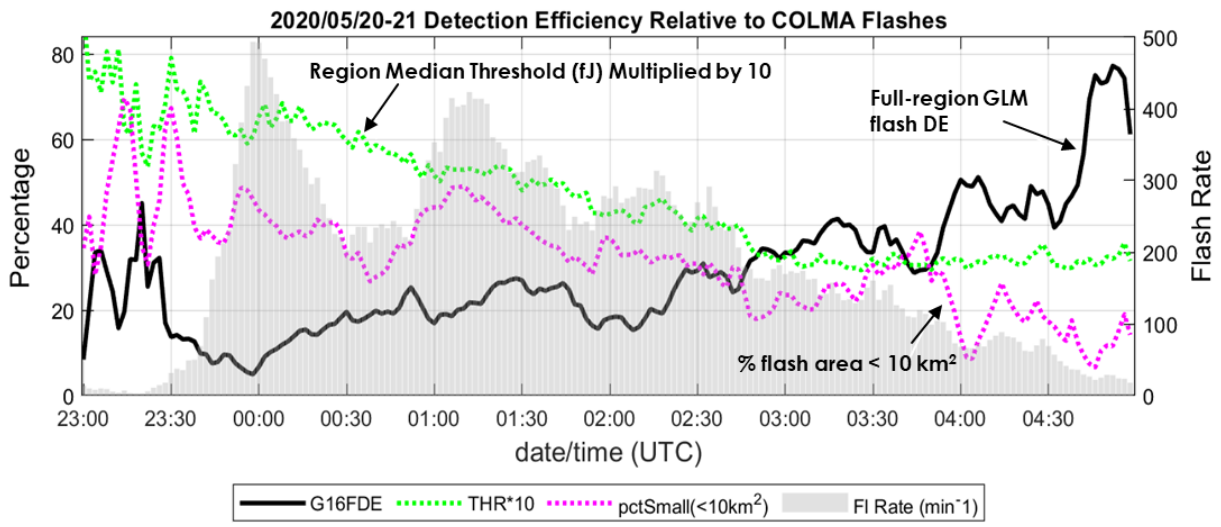

Fig. 13. Time evolution of regional lightning parameters for the region shown in Fig. 12.

4. SUMMARY AND CONCLUSIONS

This work presents the results of recent efforts to better understand and describe the performance of GLM for both the GOES-East and GOES-West locations, with the objective of assuring informed use of these important datasets. GLM flash detection efficiency (DE) is determined by the distribution of cloud-top optical energy for the brightest sources in each flash, interacting with the instrument's detection threshold. Detection threshold was shown to vary considerably by region and time-of-day. Cloud-top optical source distributions derived using historical data from the LIS sensors were also shown to vary by region, but were consistent from year to year. An approach to DE modeling was described, and validation results vs. lightning data using the Lightning Mapping Array in Florida matched the model quite well. FOV estimates of flash DE were derived for the GOES-East and -West instruments employing a CONUS-average optical source distribution, and likely local deviations of about +/-10% were noted and justified. The DE model was also used to evaluated the best possible flash DE in the CONUS region with overlapping GOES-East and -West coverage. An area of compromised performance in the north-western central plains was identified. Finally, a case study in Colorado demonstrated the practicality and value of real-time tracking of GLM detection threshold.

Future work will focus on (1) producing full field-of-view estimates of GLM flash DE that incorporate regionally-appropriate optical source distributions, and (2) exploring the best way to get this information into the hands of the operational and research communities.

Acknowledgments

The author acknowledges GHRC for providing GLM and LIS data. LMA data were provided by Jennifer Wilson, Robert Brown (NASA) and Bill Rison (New Mexico Tech). I thank NASA for continued support for this work. Helpful discussions and support throughout this work have been provided by Bill Koshak, Eric Bruning, and Daile Zhang.

REFERENCES

Bateman, M & D.M. Mach (2020): Preliminary detection efficiency and false alarm rate assessment of the Geostationary Lightning Mapper on the GOES-16 satellite, J. Appl. Remote Sens. 14(3), 032406 (2020). https://doi.org/10.1117/1.JRS.14.032406

Beirle, S., W. Koshak, R. Blakeslee, and T. Wagner (2014): Global patterns of lightning properties derived by OTD and LIS, Nat. Hazards Earth Syst. Sci., 14, doi:10.5194/nhess-14-2715-2014.

Blakeslee, R. J., Lang, T. J., Koshak, W. J., Buechler, D., Gatlin, P., Mach, D. M., et al. (2020): Three years of the Lightning Imaging Sensor onboard the International Space Station: Expanded global coverage and enhanced applications. Journal of Geophysical Research: Atmospheres, 125, e2020JD032918. https://doi.org/10.1029/2020JD032918

Boccippio, D.J., Koshak, W.J., Blakeslee, R.J. (2002), Performance assessment of the Optical Transient Detector and Lightning Imaging Sensor, I, predicted diurnal variability. J. Atmos. Oceanic Technol. 19, 1318–1332.

Bruning, E.C. and D.R. MacGorman, 2013: Theory and observations of controls on lightning flash size spectra. *Journal of the Atmospheric Sciences*, *70*(12), 4012-4029.

Chmielewski, V. C., & Bruning, E. C. (2016). Lightning mapping Array flash detection performance with variable receiver thresholds. Journal of Geophysical Research: Atmospheres, 121, 8600–8614. https://doi.org/10.1002/2016JD025159

Goodman, S.J., R.J. Blakeslee, W.J. Koshak, D. Mach, J. Bailey, D. Buechler, L. Carey, C. Schultz, M. Bateman, E. McCaul Jr, and G. Stano, (2013), The GOES-R geostationary lightning mapper (GLM). *Atmospheric research*, *125*, 34-49.

Kpulun, T, H. Demroff, C. Tillier, S. Edgington, 2021: Geostationary Lightning Mapper: Improvements for GOES-T, paper 3.9, AMS 101st Annual Meeting.

Mach, D. M. (2020): Geostationary Lightning Mapper clustering algorithm stability. Journal of Geophysical Research: Atmospheres, 125, e2019JD031900. https://doi.org/10.1029/2019JD031900

Murphy, M. J., & Said, R. K. (2020), Comparisons of lightning rates and properties from the U.S. National Lightning Detection Network (NLDN) and GLD360 with GOES-16 Geostationary Lightning Mapper and Advanced Baseline Imager data. Journal of Geophysical Research: Atmospheres, 125, e2019JD031172. https://doi.org/10.1029/2019JD031172

Quick, M.G., Christian, H.J., Virts, K.S., Blakeslee, R.J. (2020), Airborne radiometric validation of the geostationary lightning mapper using the Fly's Eye GLM Simulator, J. Appl. Remote Sens., 14(4), 044518 (2020).

Rudlosky, S. D., Goodman, S. J., Virts, K. S., & Bruning, E. C. (2019). Initial geostationary lightning mapper observations. Geophysical Research Letters, 46, 1097–1104. https://doi.org/10.1029/2018GL081052

Rutledge, S. A., Hilburn, K. A., Clayton, A., Fuchs, B., & Miller, S. D. (2020), Evaluating Geostationary Lightning Mapper flash rates within intense convective storms. Journal of Geophysical Research: Atmospheres, 125, e2020JD032827. https://doi.org/10.1029/2020JD032827

Thomas, R.J., P.R. Krehbiel, W. Rison, S.J. Hunyady, W.P. Winn, T. Hamlin, and J. Harlin, 2004: Accuracy of the lightning mapping array. *Journal of Geophysical Research: Atmospheres*, *109*(D14).

Thomas, R.J., P.R. Krehbiel, W. Rison, D.R. MacGorman, E.C. Bruning, and M.A. Stanley, 2019: Evaluation of the GOES-R Geostationary Lightning Mapper (GLM) Using Ground-Based Lightning Mapping Array (LMA) Observations. *99th American Meteorological Society Annual Meeting*, Phoenix, AZ.

Zhang, D., Cummins, K. L., Bitzer, P. M., & Koshak, W. J. (2019). Evaluation of the performance characteristics of the lightning imaging sensor. Journal of Atmospheric and Oceanic Technology, 36(6), 1015–1031. https://doi.org/10.1175/JTECH-D-18-0173.1

Zhang, D. & Cummins, K. L. (2020), Time evolution of satellite-based optical properties in lightning flashes, and its impact on GLM flash detection. Journal of Geophysical Research: Atmospheres, 125, e2019JD032024. https://doi.org/10.1029/2019JD032024